Comparative Plasma Chemical Reaction Studies of CH4/Ar and C2Hm/Ar (m = 2,4,6) Gas Mixtures in a Dielectric Barrier Discharge

ARTICLE *in* BEITRÄGE AUS DER PLASMAPHYSIK · SEPTEMBER 2014

Impact Factor: 0.84 · DOI: 10.1002/ctpp.201300035

5 AUTHORS, INCLUDING:

Thejaswini H C
Portland State University
7 PUBLICATIONS **28** CITATIONS
SEE PROFILE

Ulrike Martens
University of Greifswald
8 PUBLICATIONS **8** CITATIONS
SEE PROFILE

Rainer Hippler
University of Greifswald
331 PUBLICATIONS **3,411** CITATIONS
SEE PROFILE

Comparative Plasma Chemical Reaction Studies of CH_4/Ar and C_2H_m/Ar ($m = 2, 4, 6$) Gas Mixtures in a Dielectric Barrier Discharge.

H.C. Thejaswini, Sandra Peglow, Ulrike Martens, Vladimir Sushkov, and **Rainer Hippler***

Institut für Physik, Ernst-Moritz-Arndt-Universität Greifswald, Felix-Hausdorff-Str. 6, 17489 Greifswald, Germany

Received 15 November 2003, revised 30 November 2003, accepted 2 December 2003
Published online 3 December 2003

Key words Dielectric barrier discharge, hydrocarbon plasma chemistry, mass spectrometry, infrared spectroscopy

Plasma chemical reactions in CH_4/Ar and C_2H_m/Ar ($m = 2, 4, 6$) gas mixtures in a dielectric barrier discharge at medium pressure (300 mbar) have been investigated. From mass spectrometry the production of H_2 and formation of larger hydrocarbons such as C_nH_m with up to $n = 12$ is inferred. Hydrogen release is most pronounced for CH_4 and C_2H_6 gas mixtures. Fourier Transform InfraRed (FTIR) spectroscopy reveals the formation of substituted alkane (sp^3), alkene (sp^2), and alkyne (sp) groups from the individual gases which are used in this work. Abundant formation of acetylene occurs from C_2H_4 and to a lesser extent from C_2H_6 and CH_4 precursor gases. The main reaction pathway of acetylene leads to the formation of large molecules via C_4H_2 and, eventually, to nano-size particles. The experimental results are in reasonable agreement with simulations which predict a pronounced electron temperature and gas pressure dependency.

Contrib. Plasma Phys. 54, 683 (2014) / DOI 10.1002/ctpp.201300035

1 Introduction

Dielectric barrier discharges (DBD) have attracted much interest in recent years. The DBD was introduced by Siemens already in 1857 for ozone synthesis [1]. Applications of DBD plasmas include gas chemistry [2, 3, 4, 5], tholin formation [6, 7], fuel processing [8], sterilization [9], surface modification [10], activation [11], decontamination [12], and thin film deposition [13]. The development of new processes based on this discharge needs a clear understanding of plasma physics and chemistry. Much attention is paid to the chemical processes in barrier discharge plasma in various gas mixtures as the understanding of these processes is necessary for the development of industrial reactors [5, 14]. Besides, hydrocarbons are used for the formation of diamond-like carbon (DLC) or amorphous hydrogenated carbon (a-C:H) films and in plasma polymerization [15, 16, 17]. Hydrocarbons play an important role in the chemistry of planetary (e.g., Earth, Titan) atmospheres and they contribute to the greenhouse effect [2].

Previous investigations of plasma chemical reactions in hydrocarbon plasmas have been performed at both low and medium to atmospheric pressures. Several low pressure studies have elucidated details of the plasma chemical reaction pathways leading, e.g., to dust particle [18, 19, 20, 21, 22] and carbon nanotube formation [23]. Plasma chemical reactions in DBD plasmas were studied by, e.g., Yun Yang [24], Pietruska and Heintze [25], Majumdar et al. [26], Thejaswini et al. [27], and Kolb et al. [28]. Detailed modeling of hydrocarbon chemistry has been carried for laboratory plasmas [26, 29, 30, 31, 32] and for planetary atmospheres, e.g., Titan [6, 7, 33, 34]

In this communication we present a comparative study of plasma chemical reactions of a DBD plasma in CH_4/Ar and C_2H_m/Ar ($m = 2, 4, 6$) gas mixtures. The aim of our work is to study the discharge properties of C_2H_m/Ar ($m = 2, 4, 6$) gas mixtures in a DBD medium, the influence of the plasma on hydrocarbon gases, and a comparison of the experiment with simulation results. Detailed information about the underlying plasma

* Corresponding author: e-mail: hippler@physik.uni-greifswald.de, Phone: +49 3834 86 4780, Fax: +49 3834 86 4701

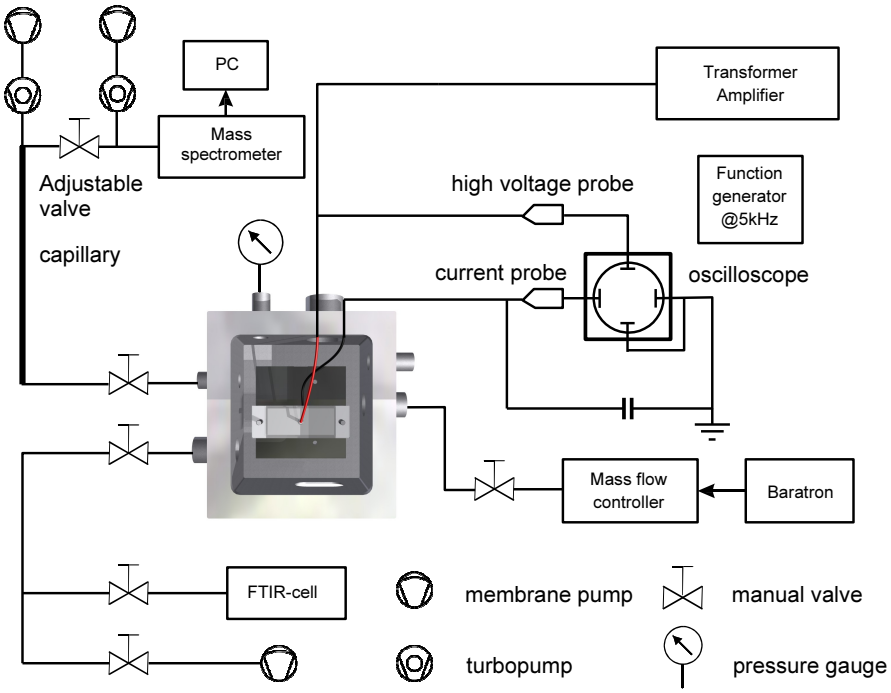

Fig. 1 Experimental set-up (schematic).

chemistry is obtained from mass spectrometry, Fourier transform infrared (FTIR) spectroscopy, and laser absorption spectroscopy. Mass spectrometry provides valuable information with regard to the formation of larger chain and/or aromatic species which are produced by plasma polymerization. A unique chemical identification is generally not possible by this method, however. Complementary details about the chemical structure of generated molecules are obtained from FTIR spectroscopy. FTIR and laser absorption spectroscopy are sensitive to functional groups in particular molecules and in many cases allow for a unique identification of a particular molecule.

2 Experimental set-up

The experimental set up has been described before [27, 26, 35]. Very briefly, it consists of a plasma chamber with inner dimensions for height, length and width of 12.3 cm, 18.0 cm, and 15.0 cm, respectively (figure 1). The two electrodes are made from stainless steel plates with a length of 8.3 cm, width 3.3 cm, and thickness 0.15 cm. The upper (powered) electrode is covered with aluminium oxide ($\epsilon \approx 10$). The lower electrode is covered with a glass plate ($\epsilon = 3.8$); it is connected to ground via a 10 nF capacitor. Both electrodes are separated by 0.15 cm from each other. The chamber is pumped by a membrane pump down to about 10 mbar. Pressure inside the plasma chamber is controlled by two gas flow controllers for the hydrocarbon and nitrogen gases and by an adjustable needle valve between the chamber and the membrane pump. The experiments are performed at a pressure of 300 mbar and with the gas flow switched off.

The high voltage power supply consists of a frequency generator delivering a sinusoidal output that is amplified by an audio amplifier and fed into a spark plug transformer. Experiments are performed at 5.7 kV and at 5.5 kHz. In order to measure the discharge power a small capacitor ($C = 10$ nF) is placed in series between the lower electrode and ground. The voltage applied to the powered electrode is measured with a high voltage probe and together with the voltage at the lower electrode serves as x and y inputs of a digital oscilloscope. The discharge power (about 3–5 W) is calculated from the resulting Lissajous figure using the standard method based on the area enclosed by the curve [36] and is kept constant during the experiments.

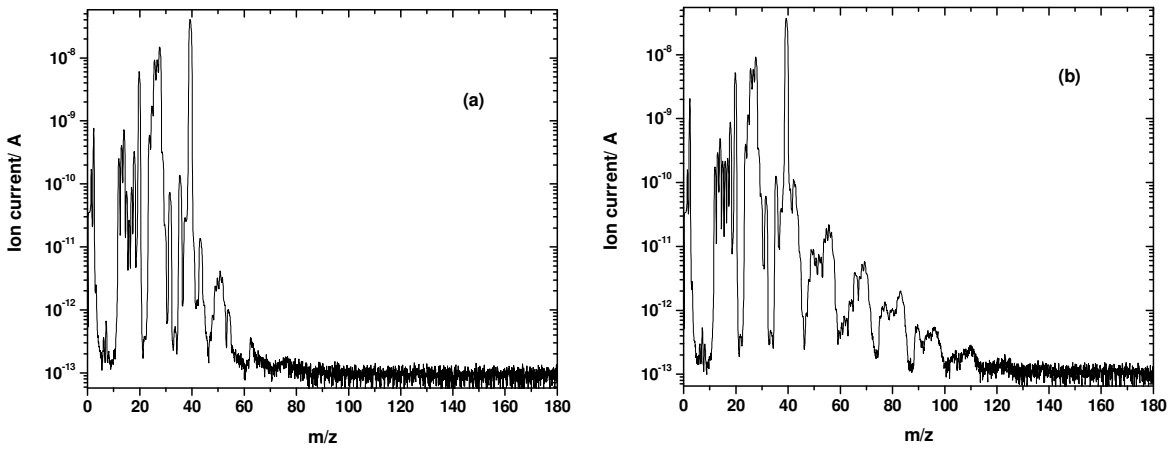

Fig. 2 Mass spectra obtained with a C_2H_4/Ar gas mixture (a) without plasma and (b) after 420 min with plasma on. Gas pressure 300 mbar, gas mixing ratio 1:2.

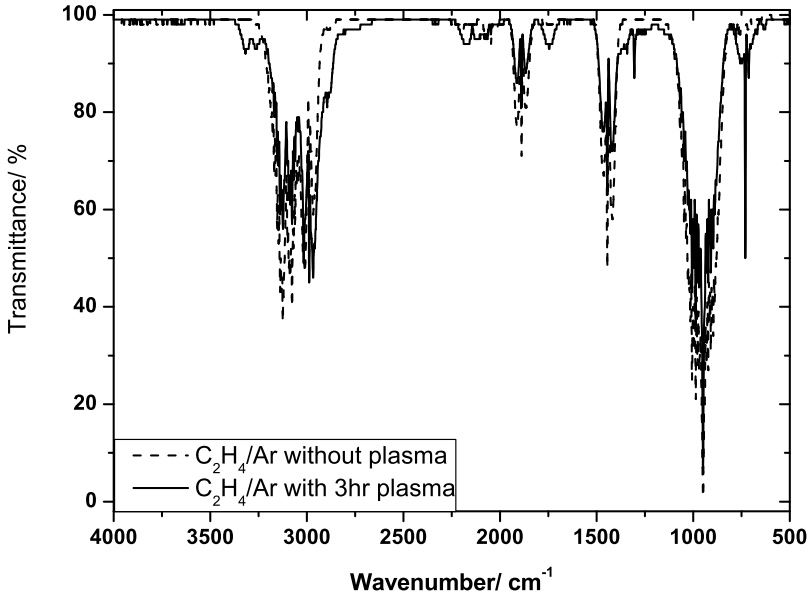

Fig. 3 FTIR spectra of C_2H_4/Ar gas mixture. Solid line: with plasma on for 180 mins, dashed line: without plasma. Gas pressure 300 mbar, C_2H_4:Ar mixing ratio 1:2.

Gas composition of stable reaction products only is monitored by a mass spectrometer (Balzers QMS 200). It is pumped by a turbomolecular pump (Pfeiffer TSU 062H) to a base pressure of about 1×10^{-8} mbar increasing to about 10^{-6} mbar during the experiment. A capillary tube of length 103 cm and inner diameter 0.01 cm connects the mass spectrometer with the plasma chamber. A pressure of 10^{-2} mbar at the entrance to the mass spectrometer is maintained during the experiments with the help of a second turbomolecular pump (Balzers 071P). Gas composition is continuously monitored. Mass spectra were taken every hour at typical sampling rates of 1 mass number per second.

Figure 2 show two typical mass spectra in the range of mass number up to $m/z = 180$ which were obtained after the chamber has been filled with 300 mbar of a C_2H_4/Ar gas mixture (mixing ratio 1:2). Figure 2(a) represents the initial gas composition consisting of argon and ethylene (C_2H_4) gas. Impurities that are present consists, e.g., of water (H_2O, $m/z = 18$), oxygen (O_2, $m/z = 32$), and small amounts of higher hydrocarbons

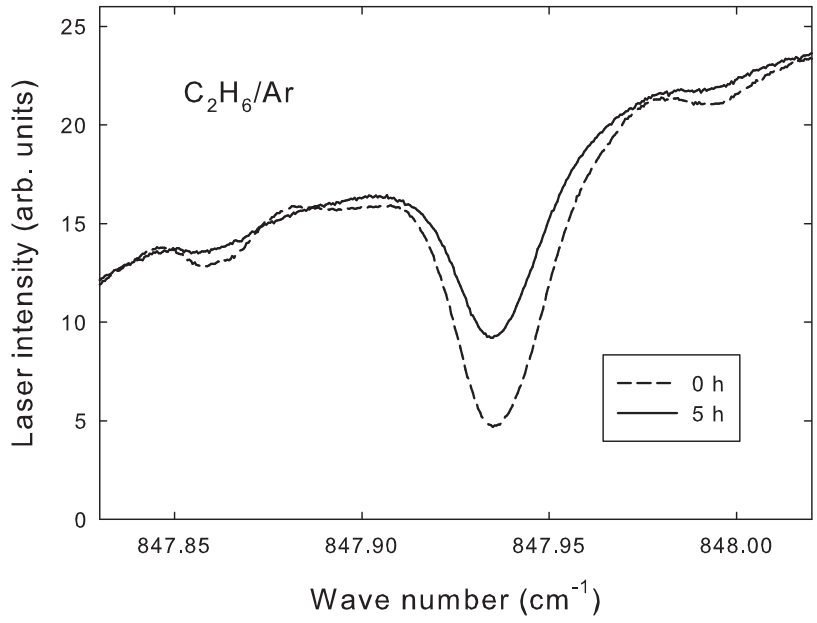

Fig. 4 Laser intensity scan *versus* wavenumber for a C_2H_6/Ar gas mixture without discharge (dashed line) anad after 5 h with discharge *on* (solid line).

around mass numbers $m/z = 50 - 57$ and 78. Stable molecules dissociate inside the ion source of the mass spectrometer, giving rise to the formation of radical ions that complicate the data analysis [37, 38]. For example, ethane with mass number 30 shows up in the mass spectra with masses $m/z = 12$ (C^+), 13–15 (CH_n^+, $n = 1-3$), 24 (C_2^+), and 25–30 ($C_2H_n^+$, $n = 1 - 6$). Hexane ($m = 86$), on the other hand, prominently shows up at mass numbers $m/z = 27$, 29, 41–43, 56, 57, and, only weakly (with about 4%), at $m/z = 86$. Information about fragmentation patterns have been obtained from the NIST Chemistry WebBook [39].

Figure 2(b) displays the mass spectrum obtained from the same gas after the discharge has been operated for 420 mins. Long operation time has been chosen because of the small discharge power of 3–5 W consumed by the plasma. Several differences compared to figure 2(a) are noted: (i) a reduction of ethylene peaks, (ii) an increase of the hydrogen peak, and (iii) the appearance of the larger hydrocarbon peaks. The experimental results presented below are obtained by subtracting the mass spectra obtained without plasma from those obtained with plasma, e.g., by subtracting the data of figure 2(a) from those of figure 2(b).

Fourier Transform Infrared (FTIR) Spectroscopy was performed with the help of a gas cell connected to the discharge chamber. The connection is made in the path between chamber and membrane pump and in such a way that the FTIR gas cell can be evacuated separately. The FTIR gas cell is made of Pyrex glass; it is equipped with two 0.4 cm thick KBr windows at each end and with closable PTFE taps on the Pyrex cell. Length and volume of the cell are 10 cm and 132 cm^3, respectively. Before starting the experiments the cell is cleaned by a continuous flow of N_2 for about 10–15 mins to remove all impurities. Then the cell is connected to the discharge chamber. The cell is pumped out by the membrane pump and then filled with the gas from the discharge chamber. FTIR analysis is performed ex-situ with the help of a FTIR spectrometer (Perkin Elmer). FTIR spectra are recorded in the range of 400–4000 cm^{-1} with a resolution of 4 cm^{-1}. The spectra presented here are obtained after subtracting the absorbance of an empty cell.

Figure 3 shows FTIR spectra for a C_2H_4/Ar gas mixture in transmittance mode. The solid line represents the C_2H_4/Ar FTIR spectrum without plasma while the dotted line represents the same gas mixture after the plasma has been operated for 180 mins. Without plasma we observe pronounced absorptions at wavenumbers 3106 cm^{-1}, 2989 cm^{-1}, 1887 cm^{-1}, 1444 cm^{-1}, and 949 cm^{-1} which are related to C–H asymmetric and symmetric stretching, scissoring, and wagging vibrations of C_2H_4 [40]. After plasma ignition we observe several additional bands at other wavenumbers. The appearance of these peaks will be discussed in the next section.

Tunable laser absorption spectroscopy (LAS) was performed for CH_4/Ar and C_2H_6/Ar gas mixtures. LAS is a powerful technique offering high resolution compared to conventional FTIR spectroscopy. Limitations are the narrow spectral range and the comparatively high costs. We have employed a commercial solid-state quantum cascade laser system (QMACS, Neoplas Control) for the absorption measurements [41]. The central laser frequency (wave number) of the is 847.9 cm^{-1}. The in-situ measurements were performed in a slightly different plasma chamber employing the same electrode configuration and power supply system. The inter-electrode separation was set to 0.2 cm. The plasma chamber was equipped with two KBr windows placed opposite with respect to each other. Typical frequency scans for the C_2H_6/Ar gas mixture are shown in figure 4. The figure displays two scans taken without discharge (0 h) and after 5 h with discharge *on*. The spectrum shows a pronounced absorption due to C_2H_6 at 847.93 cm^{-1}. Absorption spectroscopy is based on the Beer-Lambert law

$$I = I_0 \exp\left(-\kappa\, n_m\, l\right) \tag{1}$$

where I and I_0 are the measured laser intensities with and without absorbing molecules, respectively, κ is the absorption coefficient, l is the absorption length, and n_m is the absorbing molecule density (gas pressure). The total absorption is obtained by subtracting a 2^{nd} order polynomial as a base line and by numerical integration over the absorption profile. Absolute calibration is performed by in-situ absorption measurement for known gas pressure.

3 Results

In the following we separately present our results obtained from mass spectrometry, FTIR spectroscopy for CH_4/Ar, C_2H_2/Ar, C_2H_4/Ar, and C_2H_6/Ar gas mixtures.

3.1 CH_4/Ar

Mass spectra of CH_4/Ar where already presented by Majumdar et al [26]; they show the formation of C_2H_m ($m = 2, 4, 6$) and of larger hydrocarbons. FTIR spectra of CH_4/Ar gas mixture are displayed in figure 5. Figure 5(a) displays bands at 1306 cm^{-1} (1215–1380 cm^{-1}) and 3019 cm^{-1} (2900–3150 cm^{-1}) which correspond to C–H bending and stretching vibrations, respectively, of CH_4 [42]. After ignition of the plasma for 180 mins, the CH_4 concentration decreases due to consumption by the discharge and several new peaks appear. Difference FTIR plots are obtained by subtracting the data obtained with plasma from the data without plasma. Formation of C_2H_2 is inferred from the bands at wavenumbers 732 cm^{-1} and 3240–3295 cm^{-1} which correspond to C–H bending and stretching vibrations, respectively, of that molecule, see figure 5(b). The bands at wavenumbers 2900–3008 cm^{-1}, 1390–1518 cm^{-1}, and 949 cm^{-1} are related to C–H stretching vibrations, C–H deformations, and out-of-plane C–H deformations, respectively, of C_2H_4 and C_2H_6 molecules which form in the plasma. A small band at 670 cm^{-1} indicates formation of aromatic C_6H_6. Other small bands at 1746 cm^{-1} (1680–1840 cm^{-1}) and 2150 cm^1 (2045–2240 cm^{-1}) are attributed to the formation of acetaldehyde (C_2H_4O) and carbon monoxide (CO), respectively. We believe that the molecules result from the plasma interaction with oxygen-containing surfaces, e.g., electrodes.

3.2 C_2H_2/Ar

Difference mass spectra of the C_2H_2/Ar gas mixture in the mass number range m/z up to 35 and 45–180 are displayed in figure 6. Figure 6(a) shows the expected consumption of acetylene (C_2H_2) of about 60% of the initial supply during 180 min and the production of a small amount of hydrogen of about 5% of the consumed C_2H_2. A rather small amount of the consumed C_2H_2 is used for the production of larger hydrocarbons which show up at mass numbers $m/z = 48 - 50$ (butadiyne, C_4H_2), 74 (hexatriyne, C_6H_2 [39]), 78 (benzene and/or hexadiyne, C_6H_6), 92 (toluene, C_7H_8) [43]. Other peaks show up at mass numbers $m/z = 52$ (C_4H_4), 54 (C_4H_6), 56 (C_4H_8), 64 (C_5H_4). In particular the latter assignments are somewhat speculative as the fragmentation pattern of many molecules is not properly known.

The broad peak at $m/z = 64 - 68$ indicates formation of chain molecules like pentadiyne (C_5H_4), 1-penten-3-yne (C_5H_6), and pentadiene (C_5H_8), and/or cyclic molecules like cyclopentadiene (C_5H_6), cyclopropylacetylene (C_5H_6), and cyclopentene (C_5H_8). The peaks at $m/z = 78$ and 91–92 are attributed to the formation of aromatic

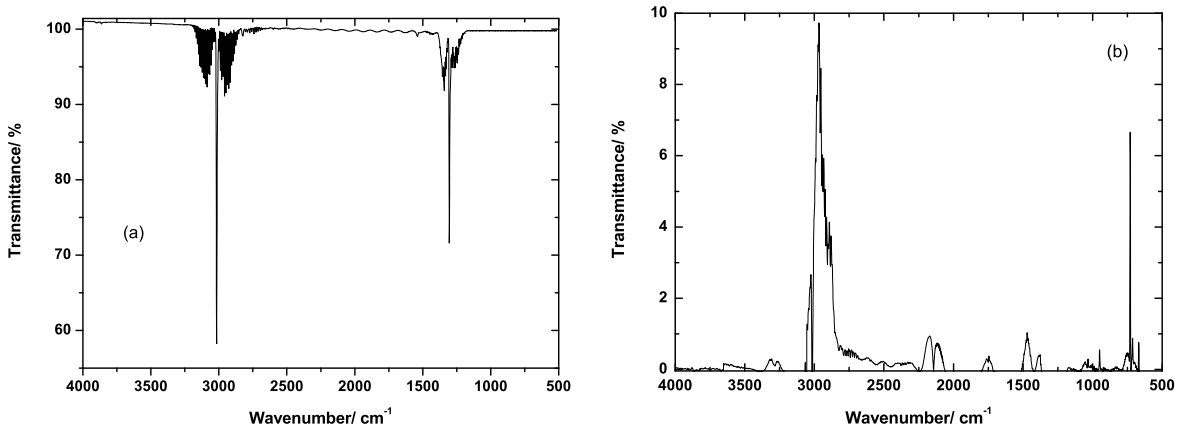

Fig. 5 FTIR spectrum of a CH_4/Ar gas mixture. (a) without plasma, (b) difference spectrum obtained by substracting the spectrum after 180 mins with plasma on from the FTIR spectrum without plasma. Gas pressure 300 mbar, gas mixing ratio 1:2, cell pressure reduced to 50 mbar.

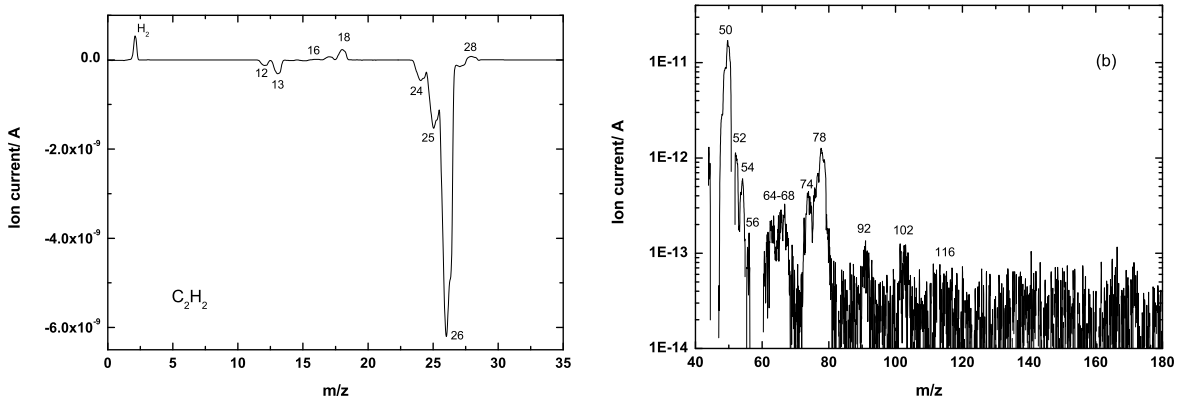

Fig. 6 Difference mass spectrum with and without plasma in the mass range m/z up to 35 (left) and 40–185 (right) for a C_2H_2/Ar gas mixture. Gas pressure 300 mbar, gas mixing ratio 1:2, plasma operation time 180 min. Note the different (linear and logarithmic) scales.

benzene (C_6H_6) and toluene (C_7H_8) molecules. Formation of aromatic compounds like phenylethyne (C_8H_6) and styrene (C_8H_8) is indicated by the peaks at mass numbers $m/z = 102 - 104$.

The FTIR spectrum of C_2H_2 is displayed in figure 7(a). It shows strong peaks at wavenumbers of 3290 cm^{-1}, 1320 cm^{-1}, and 730 cm^{-1} which are related to C–H stretching and C–H deformation vibrations of C_2H_2 [40]. After ignition of the plasma several new peaks appear in the spectrum as shown in figure 7(b). The pronounced peak at wavenumber 630 cm^{-1} and the small peak at wavenumber 1250 cm^{-1} are due to formation of biacetylene (butadiyne, C_4H_2) [44] which is also identified in the mass spectrum. CO formation by plasma-wall interaction is observed at 2150 cm^1 (2045–2240 cm^{-1}). Both molecules were also identified in the mass spectrum. The small peak at 950 cm^{-1} indicates formation of C_2H_4. Aromatic compounds like benzene are not detected in the FTIR spectrum. According to the mass spectrum, production of aromatic molecules contributes less than 10^{-3} of the consumed C_2H_2 which is below the present FTIR detection limit.

3.3 C_2H_4/Ar

Difference mass spectra from the C_2H_4/Ar gas mixture in the mass number ranges m/z up to 35 and 40–170 are displayed in figure 8. The spectrum shows the expected consumption of about 60% of the initial ethylene (C_2H_4)

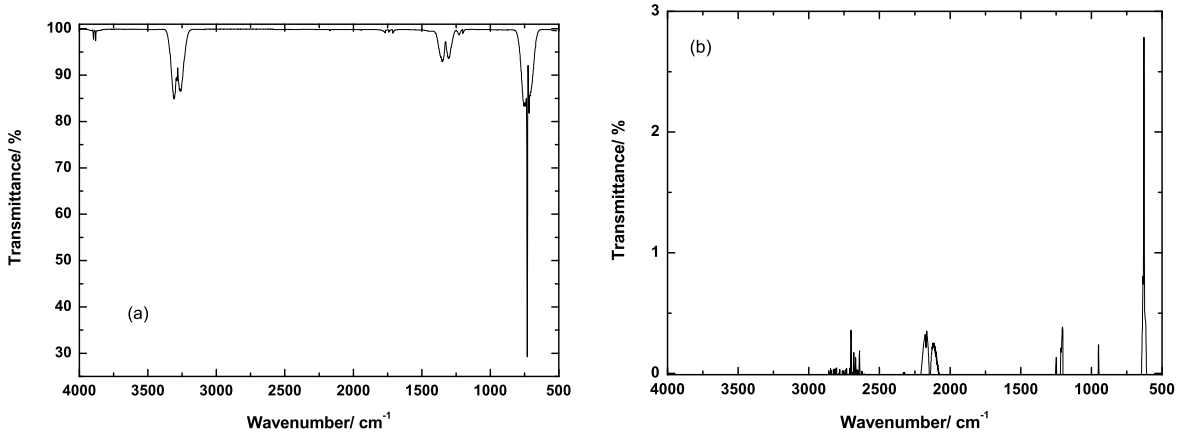

Fig. 7 FTIR spectrum of a C_2H_2/Ar gas mixture. (a) without plasma, (b) difference spectrum obtained by substracting the spectrum after 180 mins with plasma on from the FTIR spectrum without plasma. Gas pressure 300 mbar, gas mixing ratio 1:2, cell pressure reduced to 50 mbar.

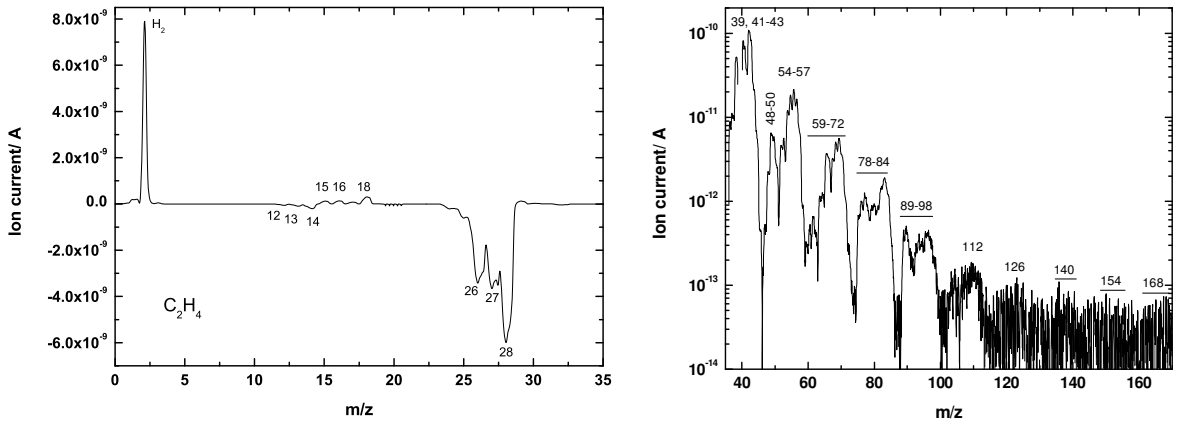

Fig. 8 Difference mass spectrum with and without plasma in the range m/z up to 35 (left) and 35–170 (right) for a C_2H_4/Ar gas mixture. Plasma operation time 420 min. Note the different (linear and logarithmic) scales.

gas. The (negative) peaks at $m/z = 12 - 14$ are related to the C, CH, and CH_2 fragments of the consumed C_2H_4. The production of a significant amount of hydrogen which corresponds to about 38% of the consumed C_2H_4 is noted. Formation of CH_4 has been identified at mass numbers $m/z = 15 - 16$. Formation of a small amount of water (H_2O) is noted by the peaks at $m/z = 17$ and 18. We believe that the water results from the plasma interaction with oxygen-containing surfaces, e.g., the electrodes.

A certain amount of the consumed C_2H_4 is used for the production of larger hydrocarbons. Hydrocarbon fragments with mass numbers up to $m/z \approx 140$ are observed. The spectrum shows several prominent groups which are separated by $\Delta m \approx 14$ corresponding to a CH_2 group. Evidently, one CH_2 radical is adding up in consecutive reactions leading to a periodic mass spectrum. The actual reaction pathways are more complicated, however, and may involve other radicals as well. Evidence for the formation of aromatic compounds like benzene (C_6H_6), methyl-benzene or toluene (C_7H_8), and ethylbenzene (C_8H_{10}) is noted as side-peaks at $m/z = 78$, 92, and 106, respectively.

Figure 9(a) shows a FTIR spectrum of the C_2H_4/Ar gas mixture. Pronounced absorptions at wavenumbers 3106 cm^{-1}, 2989 cm^{-1}, 1887 cm^{-1}, 1444 cm^{-1}, and 949 cm^{-1} are attributed to that molecule [40]. The difference spectrum displayed in figure 9(b) shows several additional peaks formed as a result of the plasma. Absorption due to methane (CH_4) is observed at wavenumbers 1306 cm^{-1} and in the 2900–3000 cm^{-1} region.

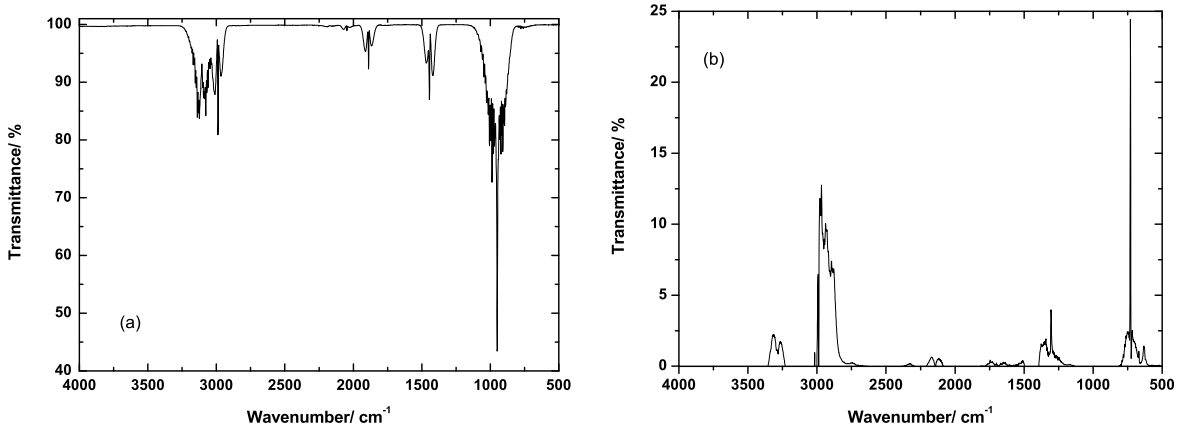

Fig. 9 FTIR spectrum of a C_2H_4/Ar gas mixture. (a) without plasma, (b) difference spectrum obtained by substracting the spectrum after 180 mins with plasma on from the FTIR spectrum without plasma. Gas pressure 300 mbar, gas mixing ratio 1:2, cell pressure reduced to 50 mbar.

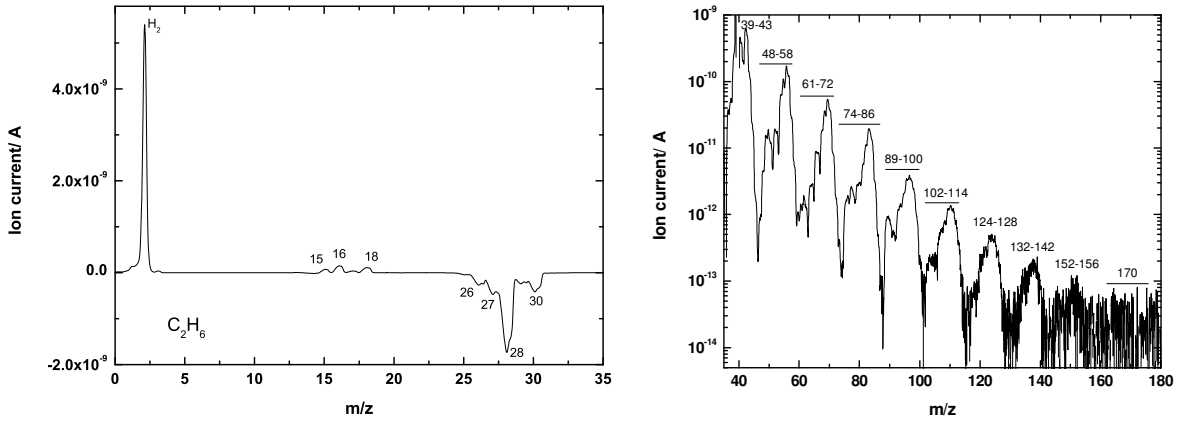

Fig. 10 Difference mass spectrum with and without plasma in the range m/z up to 35 (left) and 35–180 (right) for a C_2H_6/Ar gas mixture. Plasma operation time 360 min. Note the different (linear and logarithmic) scales.

The later region is difficult to quantify since the bands of CH_4 and C_2H_6 partly overlap with C_2H_4. Pronounced absorptions due to acetylene (C_2H_2) are detected at wavenumbers 732 cm^{-1} and 3300 cm^{-1}. Formation of biacetylene (C_4H_2), albeit small, is observed at wavenumber 630 cm^{-1}. The tiny band at 2150 cm^1 is attributed to the formation of molecules with C=O bonds (e.g., CH_2O, C_2H_4O) presumably by reactions with oxygen-containing impurities from the chamber's electrodes and walls.

3.4 C_2H_6/Ar

Figure 10(a) displays the measured difference mass spectrum for mass numbers up to $m/z = 35$ on a linear scale obtained by subtracting the data without plasma from those obtained with plasma after 360 min. The production of hydrogen (H_2) and methane (CH_4) and a significant consumption of ethane, the latter corroborated by the (negative) ethane peaks at $m/z = 25 - 30$, becomes evident. The most abundant fragment ion of ethane occurs at m/z = 28. In addition, production of larger hydrocarbons becomes evident from the mass spectrum in the range $m/z = 35 - 180$ which is displayed in figure 10(b) on a logarithmic scale. The mass spectrum is similar to the one from the C_2H_4/Ar gas mixture. The spectrum shows similar broad prominent peaks, each composed of several individual peaks, that are attributed to C_nH_m molecules with n up to 12 and $m \approx 2n + 2$. Again, the most prominent peaks, hence, approximately differ by $\Delta m \approx 14$ from each other.

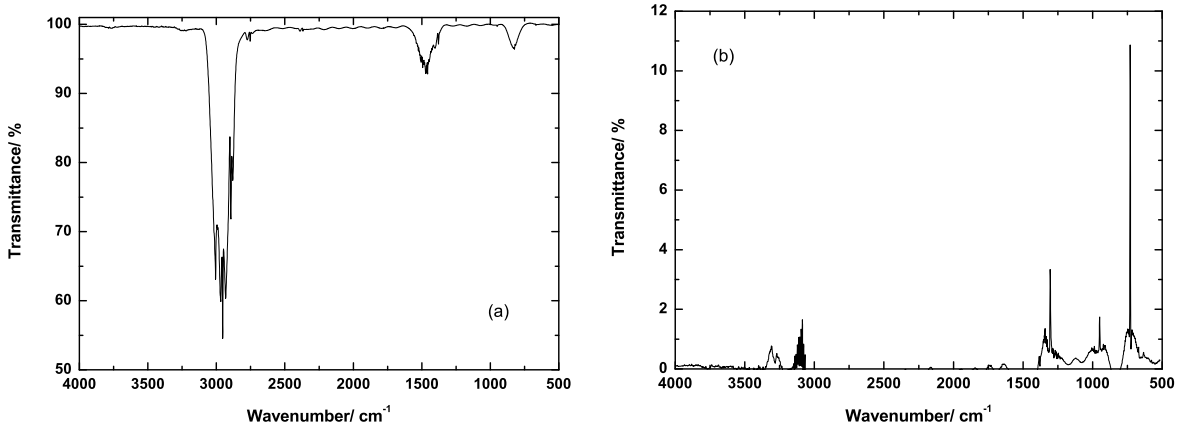

Fig. 11 FTIR spectrum of a C_2H_6/Ar gas mixture. (a) without plasma, (b) difference spectrum obtained by substracting the spectrum after 180 min with plasma on from the FTIR spectrum without plasma. Gas pressure 300 mbar, gas mixing ratio 1:2, cell pressure reduced to 50 mbar.

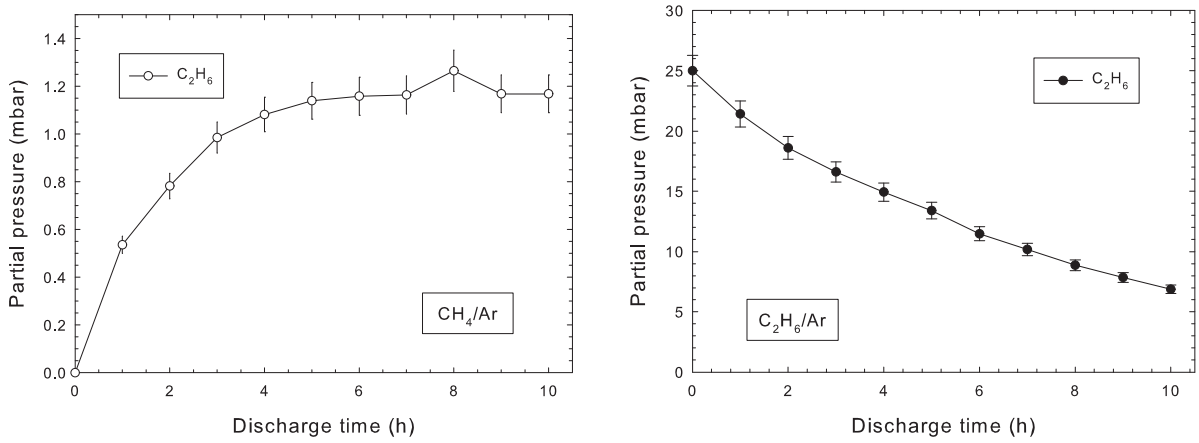

Fig. 12 C_2H_6 partial pressure *versus* discharge time for CH_4/Ar (left) and C_2H_6/Ar (right) gas mixtures. Discharge power 1.3 W and 2.8 W for CH_4/Ar and C_2H_6/Ar, respectively. Initial CH_4 and C_2H_6 partial pressure 25 mbar. Argon partial pressure 25 mr bar.

Fig. 11 shows FTIR spectra of C_2H_6/Ar gas mixture. Bands at wavenumbers 2900 cm^{-1}, 1470 cm^{-1} and 822 cm^{-1} are related to C–H stretching, deformation, and bending vibrations, respectively [40]. After ignition of the plasma several new peaks appear which are related to CH_4 (1306 cm^{-1}), C_2H_2 (732 cm^{-1} and 3300 cm^{-1}), and C_2H_4 (950 cm^{-1}).

3.5 Laser absorption measurements for CH_4/Ar and C_2H_6/Ar gas mixtures

Figure 12 displays the time dependency of the C_2H_6 partial pressure derived from the laser absorption measurements for C_2H_6/Ar and CH_4/Ar gas mixtures. A pronounced decrease of the C_2H_6 supply is noted for the C_2H_6/Ar gas mixture (right figure). The decrease is in reasonable agreement with the mass spectrometry and FTIR measurements. The left figure 12 displays the time dependency of the C_2H_6 partial pressure for the CH_4/Ar gas mixture. The discharge power was 1.3 W. A pronounced increase of the C_2H_6 partial pressure is seen which saturates at ≈ 1.2 mbar. Thus, about 5% of the initial CH_4 supply is converted into C_2H_6 at this discharge power. The total converted amount is presumably even larger as part of the produced C_2H_6 is consumed in the formation of other species.

Table 1 Percentage gas production and consumption for CH_4/Ar and C_2H_m/Ar ($m = 2, 4, 6$) gas mixtures during 180 min of DBD plasma as derived from mass spectrometry (H_2) and FTIR spectroscopy (CH_4, C_2H_2, C_2H_4, and C_2H_6). The initial hydrocarbon and argon pressure is 100 mbar and 200 mbar, respectively.

Initial	Gas consumption/production (%)				
Gas	H_2	CH_4	C_2H_2	C_2H_4	C_2H_6
CH_4	24	–34	4.5	0.4	13
C_2H_2	3	–	–60	0.3	–
C_2H_4	23	13	23	–60	23
C_2H_6	17	11	10	2.4	–19

3.6 Films

A significant fraction of the consumed gases condenses on the electrodes forming films with particular properties. Typical film colors range from dark brown (for C_2H_2) to light yellow (for C_2H_6). More details on film formation have been presented elsewhere [45].

4 Discussion

The amount of gas consumed during 180 mins of plasma operation is summarized in table 1. Numbers are obtained from mass spectrometry (H_2) and FTIR spectroscopy (CH_4, C_2H_2, C_2H_4, and C_2H_6), the latter were derived with the help of the Beer-Lambert law (Eq. 1). C_2H_2 and C_2H_4 show the largest gas consumption of about –60% followed by CH_4 with –34% and C_2H_6 with about –19%. C_2H_2 and C_2H_4 thus have the highest decomposition rates of the investigated gases in a DBD plasma. The present result is in reasonable agrement with previous observations [8].

In order to estimate the energy required to decompose a single hydrocarbon molecule we take a power consumption of 3–4 W during the experiments into account. With 50% of the initial hydrocarbon gas consumed during 180 min the energy required to break up a hydrocarbon molecule is about 45–60 eV/molecule or 4300–5800 kJ/mol.

Significant amounts of hydrogen molecules are produced by decomposition of CH_4, C_2H_4, and C_2H_6. About 0.7 and 0.9 hydrogen molecule per consumed CH_4 or C_2H_6 molecule, respectively, are produced. For C_2H_4 the corresponding number amounts to about 0.4 and is thus significantly smaller. The smallest amount of H_2 molecules is produced with the C_2H_2 gas mixture (about 0.05 H_2 per consumed C_2H_2 molecule).

Apart from rather small amounts of H_2 and C_2H_4 only a few other gases, most notably C_4H_2 ($m/z = 50$), are found in the acetylene plasma. Presumably, C_2H_2 quickly grows to large hydrogen-poor hydrocarbons outside of our detection range and/or is deposited as a film on the electrodes [45]. Possible pathways are via C_4H_2, which is the dominant new species in the FTIR spectrum, C_4H_4, C_6H_2, and C_6H_6 as is further evidenced by the observed peaks at mass numbers $m/z = 52$, 74, and 78 (figure 6). Of these, C_4H_2 and C_6H_2 are chain molecules formed by polymerization of C_2H_2, e.g., through chemical reactions involving C_2H radicals [46, 47, 48, 49],

$$C_{2n}H_2 + C_2H \rightarrow C_{2n+2}H_2 + H\,. \tag{2}$$

Chemical reactions studies during pyrolysis of C_2H_2 indicate that the corresponding reaction rates are rather large [50].

C_2H_6 formation is the dominant process in the methane plasma, as evidenced from the FTIR spectra. Taking into account that C_2H_6 contains twice as much carbon as CH_4 about 70% of the carbon is converted in this way. Much of the remaining gas (about 25%) is used for the production of C_2H_2. The result is in fair agreement with simulations of DeBie et al. [31].

C_2H_2 and C_2H_6 formation are the dominant processes and of about equal importance in the C_2H_4 plasma; roughly 35% of the available C_2H_4 gas are consumed in either way.

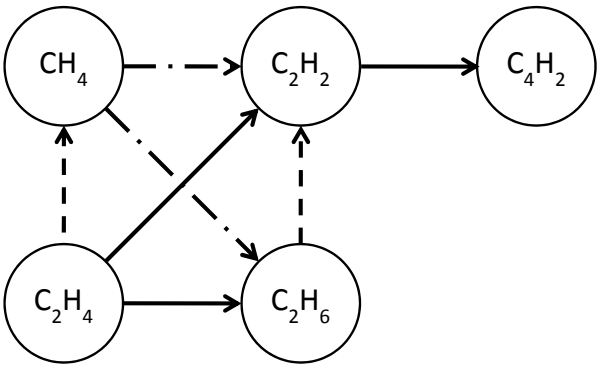

Fig. 13 Main reaction pathways among the CH_4, C_2H_2, C_2H_4, C_2H_6, and C_4H_2 molecules. Arrows indicate the net balance of *forward* (e.g., $CH_4 \rightarrow C_2H_6$) and *backward* (e.g., $CH_4 \leftarrow C_2H_6$) pathways. Strong (solid lines), medium (dashed lines), and weak (dash-dotted lines) pathways are indicated.

C_2H_2 formation is the dominant process in the C_2H_6 plasma. Roughly 55% of the consumed C_2H_6 gas is used in this way. CH_4 and C_2H_4 formation contribute about 30% and 13%, respectively, to C_2H_6 consumption.

The relative strength and the direction of the reaction pathways among the CH_4, C_2H_2, C_2H_4, and C_2H_6 molecules are summarized in figure 13. Arrows indicate the net balance of *forward* (e.g., $CH_4 \rightarrow C_2H_6$) and *backward* (e.g., $CH_4 \leftarrow C_2H_6$) pathways. It follows that C_2H_4 quickly decomposes into C_2H_2, C_2H_6 and CH_4. C_2H_2 is predominately produced from C_2H_4, moderately produced from C_2H_6 and weakly produced from CH_4. CH_4 is produced from C_2H_4 and contributes to the formation of C_2H_2 and C_2H_6.

Experimental evidence for the formation of aromatic compounds like benzene (C_6H_6), methyl-benzene or toluene (C_7H_8), and ethylbenzene (C_8H_{10}) is noted as peaks or side-peaks at $m/z = 78$, 92, and 106, respectively, in all mass spectra. Similar mass spectra were observed for C_2H_m/N_2 ($m = 2, 4, 6$) gas mixtures [27]. The similarity seem to indicate that the presence of neither excited (metastable) argon atoms [51] nor of nitrogen radicals has a strong impact on hydrocarbon chemistry.

Formation of larger C_nH_m hydrocarbons with n up to 12 is observed for all gas mixtures. Only a small fraction of about 0.6% of the consumed C_2H_2 gas is used in the formation of larger hydrocarbons, most notably C_4H_2, C_4H_4, C_6H_2, and C_6H_6. Apparently, the remaining fraction of the consumed C_2H_2 quickly grows via reaction (2) to much larger molecules outside our detection range including nano-particles [20, 52, 53] and/or is deposited as a film on the electrodes. Much larger fractions of about 23% and 15% of the consumed CH_4 and C_2H_4 gases (8% and 9% of the initial gases), respectively, are converted to larger hydrocarbons. Similarly, about 15% of the consumed gas (3% of the initial gas) are converted during plasma operation in C_2H_6. Apparently, plasma polymerization obeying a gross reaction scheme

$$C_nH_m + CH_2 \rightarrow C_{n+1}H_{m+2} \tag{3}$$

is a dominant process responsible for the periodic mass spectra from CH_4, C_2H_4, and C_2H_6 gas mixtures were the broad peaks differ by $\Delta m \approx 14$. The actual reaction schemes are more complicated, however, and may involve other radicals like CH, CH_3, C_2H, C_2H_3, C_2H_5, etc., as well.

The above results are in fair agreement with present simulations for the investigated hydrocarbon species. In order to calculate the hydrocarbon species distribution we employ the zero-dimensional particle-balance model as described recently by Matyash et al [29]. The model assumes that the plasma is uniform, electrons and ions have a Maxwellian energy distribution, and electron temperature and density and ion temperature are constant. The temporal behavior of neutral and ion species densities is calculated from a system of particle balance equations. Neutral and ion densities are assumed to change due to volume chemical reactions. In the expanded model we now account for a total of 197 volume reactions involving 18 neutral and 13 charged species: C_4H_2, C_3H_8, C_3H_6, C_3H_4, C_2H_6, C_2H_5, C_2H_4, C_2H_3, C_2H_2, C_2H, C_2, CH_4, CH_3, CH_2, CH, C, H_2, H, and $C_2H_5^+$, $C_2H_4^+$, $C_2H_3^+$, $C_2H_2^+$, CH_5^+, CH_4^+, CH_3^+, CH_2^+, CH^+, C^+, H_3^+, H_2^+, and H^+.

The present simulation results for CH_4 are in fair agreement with the advanced simulations by DeBie et al. [31]. Accordingly, stable H_2, C_2H_2, C_2H_4, C_2H_6, C_3H_m ($m = 6$, 8), and C_4H_2 molecules form in the discharge

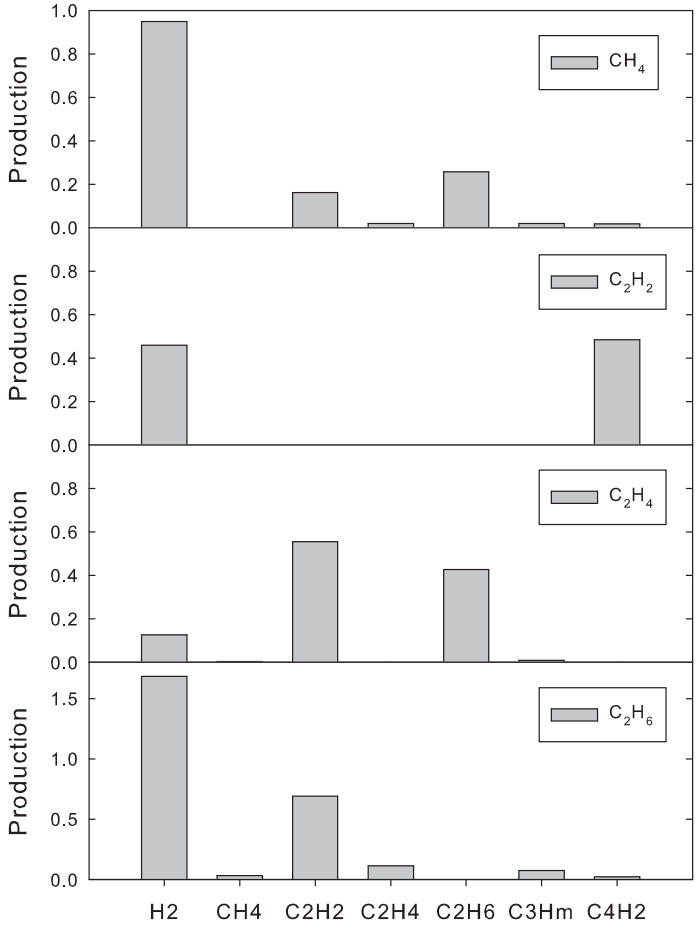

Fig. 14 Simulation results for the production (in molecules per consumed molecule) of H_2, CH_4, C_2H_2, C_2H_4, C_2H_6, C_3H_m ($m = 4, 6, 8$), and C_4H_2 molecules when half of the initial hydrocarbon gas is consumed. Electron temperature 3 eV, electron density 10^{11}/cm^3, initial species (CH_4, C_2H_2 C_2H_4, C_2H_6) density 2.8×10^{18}/cm^3.

(figure 14). Most abundant is H_2 followed by the formation of C_2H_6 and C_2H_2. The relatively small abundance of C_2H_4 is attributed to the high reactivity of this molecule. Larger hydrocarbons like C_3H_m and C_4H_2 also form through polymerization reactions. In the present simulation the latter molecules serve as end-products and no loss mechanisms for these molecules are included. C_3H_m and C_4H_2 are thus representative of all higher polymerized species not included in the simulation, as was pointed out by DeBie et al. [31].

The simulations confirm the experimental result that the CH_4 and C_2H_6 gas mixtures produce the largest amount of hydrogen. The simulation results for C_2H_2 and C_2H_4 deviate from the experimental observation. In the C_2H_2 plasma the dominant reaction leads to the formation of C_4H_2 which is the end-product of the simulation. Accordingly, two C_2H_2 molecules form one C_4H_2 molecule plus one H_2 molecule. In reality C_4H_2 continues to grow via the polymerization reaction (2) to even larger $C_{2n}H_2$ ($n \geq 3$) molecules leading to the liberation of one H_2 molecule per consumed C_2H_2 molecule. Clearly, this is not observed in the experiment. We believe that during C_2H_2 plasma operation much of the released hydrogen is bound into the forming polymer-like film on the electrodes thereby reducing the amount of free hydrogen [54].

A different situation arises for the C_2H_4 plasma. In this case the major reaction channel result in the formation of C_2H_2 and C_2H_6 molecules. Then, the amount of liberated hydrogen is to a large extent determined by the difference of the produced C_2H_2 and C_2H_6 molecules. It follows from the present simulation that the C_2H_2-to-C_2H_4 ratio and thus the amount of free hydrogen is strongly affected by the plasma parameters (figure 15). For example, the released hydrogen amount strongly increases with electron temperature and decreases with C_2H_4

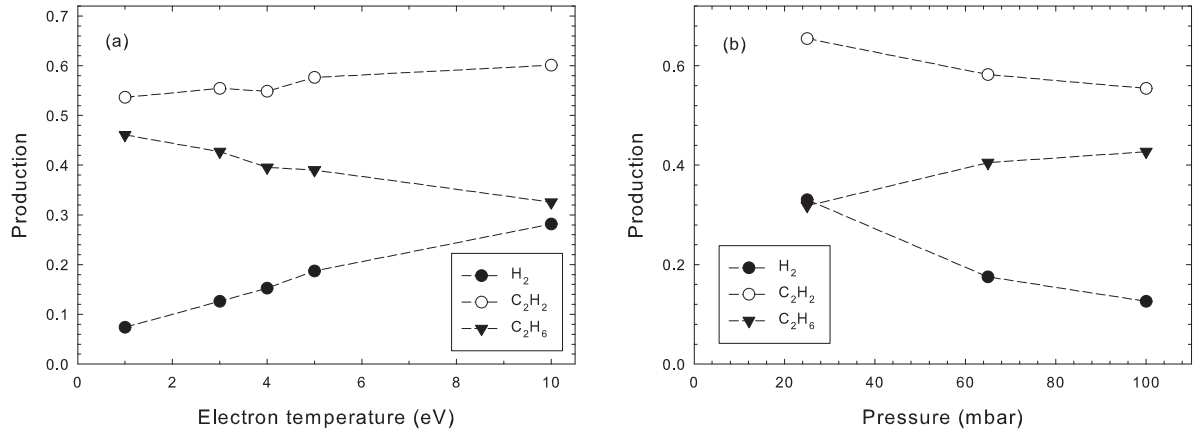

Fig. 15 Simulation results for the production of (•) H_2, (○) C_2H_2, and (▼) C_2H_6 (in molecules per consumed molecule) when half of the initial C_2H_4 gas is consumed *versus* (a) electron temperature (initial C_2H_4 gas pressure 100 mbar) and (b) C_2H_4 gas pressure (electron temperature 3 eV).

gas pressure. The comparison shows that it is possible to control plasma chemistry by a proper adjustment of plasma parameters.

5 Summary

Experimental and simulation results are presented for the break down of CH_4/Ar and C_2H_m/Ar ($m = 2, 4, 6$) gas mixtures in a dielectric barrier discharge plasma. The experiment shows that CH_4 and C_2H_6 produce the largest amount of hydrogen. The smallest amount of H_2 molecules is produced with the C_2H_2 gas mixture.

C_2H_6 formation is main reaction process in the methane plasma. C_2H_2 formation is the dominant process in the C_2H_6 plasma while C_2H_2 and C_2H_6 formation are the main processes in the C_2H_4 plasma. Acetylene quickly grows to form large molecules via bi-acetylene (C_4H_2). Significant formation of larger C_nH_m hydrocarbons with n up to 12 is observed for the CH_4, C_2H_4, and C_2H_6 gases. Typically, about 15–25% of the consumed gas are converted in this way. Apparently, plasma polymerization is a major process and responsible for the periodic mass spectra from CH_4, C_2H_4, and C_2H_6 gas mixtures were the broad peaks differ by $\Delta m \approx 14$. The experimental results are supported by simulations. The simulations further indicate the control of plasma chemistry by proper adjustment of plasma parameters.

Acknowledgements

We like to thank Dr. Abhijit Majumdar, Dr. K. Matyash, and Prof. R. Schneider for helpful discussion and support. The work was supported by the Deutsche Forschungsgemeinschaft (DFG) through SFB/TR 24 "Fundamentals of Complex Plasmas", the International Max-Plank Research School (IMPRS) for "Bounded Plasmas", and through a Landesgraduiertenstipendium provided by the University of Greifswald to one of us (HCT).

References

[1] Kogelschatz U, Plasma Chem Plasma Process 23, 1 (2003)
[2] De Bie C, Martens T, van Dijk J, Paulussen S, Verheyde B, Corthals S, Bogaerts A, Plasma Sources Sci. Technol. 20, 024008 (2011)
[3] Kolb T, Kroker T, Voigt JH, Gericke K-H, Plasma Chem Plasma Process 32, 1139 (2012)
[4] Kozlov KV, Michel P, Wagner H-E, Czech. J. Phys. 48, 1199 (1998)
[5] Kozlov KV, Michel P, Wagner H-E, Plasmas and Polymers 5, 129 (2000)
[6] Suits G, J. Phys. Chem. A 113, 11098 (2009)
[7] Cable ML, Hörst SM, Hodyss R, Beauchamp PM, Smith MA, Willis PA, Chem. Rev. 2012, 1882 (2012)

[8] Indarto A, Coowanitwong N, Choi. J-W, Lee H, Song HK, Fuel Proc. Technol. 89, 214 (2008)
[9] Jai Hyuk Choi, Inho Han, Hong Koo Baik, Mi Hee Lee, Dong-Wook Han, Jong-Chul Park, In-Seob Lee, Kie Moon Song, Yong Sik Lim, Journal of Electrostatics 64, 17 (2006)
[10] Tajima S, Komvopoulos KJ, Appl. Phys. 101, 014307 (2007)
[11] Esrom H, Seebock R, Charbonnier M, Romand M, Surface and Coatings Technology 125, 19 (2000)
[12] Laroussi M, IEEE Transactions on plasma science, Vol. 30, 1409 (2002)
[13] Dong-Wha Park, Sung-Hwan Yoon, Geon-Joong Kim, Hidetoshi Sekiguchi, J. Ind. Eng. Chem., Vol. 8, No. 4, (2002) 393-398
[14] Basner R, Foest R, Schmitt M, Hempel F, Becker K, Proc. XXIII ICPIG (Toulouse, France, July 17-22, 1997), Vol IV, p. 196 (1997); Basner R, Foest R, Schmitt M, Hempel F, Becker K, Gaseous Dielectrics, Vol VIII, L.G. Christophotou, D.R. James, Eds., New York: Plenum, p. 161 (1998)
[15] Lai-shun shi, Lu-Yan Wang, Yu-Na Wang, European Polymer Journal 42, 1625 (2006) 1625
[16] Hollenstein Ch, Plasmas and Polymers 3, 249 (1998)
[17] Inoue Y, Sugimura H, Takai O, Thin Solid Films 345, 90 (1999)
[18] Deschenaux Ch, Affolter A, Magni D, Hollenstein Ch, Fayet P, J. Phys. D: Appl. Phys. 32 (1999) 1876-1886.
[19] Hong S, Berndt J, Winter J, Plasma Sources Sci. Technol. 12, 46 (2003)
[20] Do HT, Thieme G, Fröhlich M, Kersten H, Hippler R, Contrib. Plasma Phys. 45, 378 (2005)
[21] Benedikt J, Consoli A, Schulze M, von Keudell A, J. Phys. Chem. A 111, 10453 (2007)
[22] Consoli A, Benedikt J, von Keudell A, J. Phys. Chem. A 112, 11319 (2008)
[23] Mao M, Bogaerts A, J. Phys. D 43, 205201 (2010)
[24] Yun Yang, Plas. Chem. Plas. Proc. 23, 283 (2003)
[25] Petruska B, Heintze M, Catalysis Today 90, 151 (2004)
[26] Majumdar A, Behnke JF, Hippler R, Matyash K, Schneider R, J. Phys. Chem. A 109, 9371 (2005)
[27] Thejaswini HC, Majumdar A, Tun TM, Hippler R, Advances in Space Research 48, 857 (2011)
[28] Kolb T, Voight JH, Gericke K-H, Plas. Chem. Plas. Proc. 33, 631 (2013)
[29] Matyash K, Schneider R, Bergmann A, Jacob W, Fantz U, Pecher P, J. Nucl. Mat. 434, 313 (2003)
[30] De Bleecker K, Bogaerts A, Goedheer W, Phys. Rev. E 73, 026405 (2006)
[31] De Bie C, Verheyde B, Martens T, Van Dijk J, Paulussen S, Bogaerts A, Plasma Process. Polym. 8, 1033 (2011)
[32] Takana H, Takana Y, Nishiyama H, EPL 97, 25001 (2012)
[33] Vladimir A. Krasnopolsky VA, Icarus 201, 226 (2009)
[34] T.E. Cravens TE, Robertson IP, Waite Jr. JH, Yelle RV, Vuitton V, Coates AJ, Wahlund J-E, Agren K, Richard MS, De La Haye V, Wellbrock A, Neubauer FM, Icarus 199, 174 (2009)
[35] Majumdar A, Hippler R, Rev. Sci. Instr. 78, 075103 (2007)
[36] Wagner H-E, Brandenburg R, Kozlov KV, Sonnenfeld A, Michel P, Behnke JF, Vacuum 71, 417 (2003)
[37] Boufendi L, Bouchoule A, Plasma Sources Sci. Technol. 3, 262 (1994)
[38] Boufendi L, Hermann J, Bouchoule A, Dubreuil B, Stoffels E, Stoffels WW, de Giorgi ML, J Appl. Phys. 76, 148 (1994)
[39] NIST Mass Spec Data Center, S.E. Stein, director, "Mass Spectra" in NIST Chemistry WebBook, NIST Standard Reference Database Number 69, Eds. P.J. Linstrom and W.G. Mallard, National Institute of Standards and Technology, Gaithersburg MD, 20899, http://webbook.nist.gov (retrieved June 7, 2012).
[40] NIST Mass Spec Data Center, SE Stein, director, "Infrared Spectra" in NIST Chemistry WebBook, NIST Standard Reference Database Number 69, Eds. P.J. Linstrom and W.G. Mallard, National Institute of Standards and Technology, Gaithersburg MD, 20899, http://webbook.nist.gov (retrieved June 7, 2012).
[41] Röpcke J, Davies PB, Lang N, Rousseau A, Welzel S, J. Phys. D: Appl. Phys. 45 423001 (2012)
[42] Raulin F, Accaoui B, Razaghi A, Dang-Nhu AM, Coustenis A, Gautier D, Spectrochimica Acta, Vol. 46A, 671 (1990).
[43] Wilson EH, Atreya SK, Journal of Geophysical Research 108, 801 (2003).
[44] Khlifi M, Paillous P, Delpech C, Nishio M, Bruston P, Raulin F, J. Mol. Spectrosc. 174, 116 (1995)
[45] Martens U, Thejaswini HC, Majumdar A, Hippler R, Plasma Process. Polym. 9, 647 (2012)
[46] Pedersen JOP, Opansky BJ, Leone SR, J. Phys. Chem. 97, 6822 (1993)
[47] Kovács T, Blitz MA, Seakins PW, J. Phys. Chem. A 114, 4735 (2010)
[48] Benedikt J, J. Phys. D: Appl. Phys. 43, 043001 (2010)
[49] Landera A, Krishtal SP, Kislov VV, Mebel AM, Kaiser RI, J. Chem. Phys. 128, 214301 (2008)
[50] Norinaga K, Deutschmann O, Ind. Eng. Chem. Res. 46, 3547 (2007)
[51] Riccardi C, Barni R, Fontanesi M, Tosi P, Czech. J. Phys. 50/S3, 389 (2000)
[52] Winter J, Berndt J, Hong S-H, Kovacevic E, Stefanovic I, Stefanovic O, Plasma Sources Sci. Technol. 18, 034010 (2009)
[53] Do HT, Suchkov V, Hippler R, New. J. Phys. 11, 033020 (2009)
[54] Thejaswini HC, Ph.D. thesis, University of Greifswald (2012)